What can adaptive optics do for a scanning laser ophthalmoscope ?

ROORDA A.[1], GARCIA C.A.[3], MARTIN J.A.[2], POONJA S.[1], QUEENER H.[2], ROMERO-BORJA F.[2], SEPULVEDA R.[3], VENKATESWARAN K.[1], ZHANG Y.[1]

ABSTRACT

By compensating for the aberrations in the eye that cause blur, the adaptive optics scanning laser ophthalmoscope (AOSLO) yields high-magnification, high-resolution, real-time images of the living human retina. Features as small as single cone photoreceptors can be resolved, single leukocytes are recorded in real time as they pass through the smallest retinal capillaries, and the optical sectioning capability can be used to visualize independent layers of the retinal tissue ranging from the nerve fiber layer, through the blood vessels to the photoreceptors.

The use of AO technology not only enhances the breadth of applications of conventional SLOs, but it facilitates a host of new applications. Here we provide an overview of AOSLO performance and its applications, including two clinical examples. Finally, we preview two novel applications; one where the AOSLO is used to present AO-corrected stimuli directly onto the retina while simultaneously recording their exact retinal position, and a second application where AOSLO videos are used to provide very precise, high-frequency measures of eye movements.

KEY WORDS

Scanning laser ophthalmoscope, adaptive optics, blood flow, optical sectioning, ocular aberrations, eye movements

RÉSUMÉ

En compensant les aberrations de l'œil causant un flou, l'ophthalmoscope laser à balayage à optique adaptative (OLBOA) permet d'obtenir un fort grossissement, une haute résolution, des images en temps réel de la rétine de l'humain vivant. Des éléments aussi petits que de simples photorécepteurs coniques peuvent être visibles, des leucocytes isolés sont enregistrés en temps réel quand ils passent à travers les plus petits capillaires rétiniens, et la capacité de sectionnement optique peut être utilisée pour visualiser des couches indépendantes du tissu rétinien allant de la couche de fibres nerveuses aux photorécepteurs en passant par les vaisseaux sanguins.

L'utilisation de la technologie OA n'améliore pas seulement le champ d'application des OLB conventionnels, mais facilite également une multitude de nouvelles applications. Nous fournissons ici une vue d'ensemble de la performance de l'OLBOA et de ses applications, en incluant deux exemples cliniques. Enfin, nous annonçons deux nouvelles applications : une dans laquelle l'OLBOA est utilisé pour présenter des stimuli corrigés par OA directement sur la rétine tout en enregistrant simultanément leur position rétinienne exacte, et une deuxième application dans laquelle des vidéos d'OLBOA sont utilisées pour fournir des mesures à haute fréquence très précises des mouvements oculaires.

.....

[1] *University of California, Berkeley, School of Optometry, Berkeley*
[2] *University of Houston College of Optometry, Houston TX*
[3] *University of Texas, Houston Health Science Center, Houston, TX*

MOT-CLÉS

Ophthalmoscope laser à balayage, optique adaptative, flux sanguin, sectionnement optique, aberrations oculaires, mouvements oculaires

INTRODUCTION

The invention of the scanning laser ophthalmoscope in 1980 represented one of the major developments in ophthalmoscopy in the 20 century.[21,34] It has since enjoyed widespread use and application as a tool for basic science as well as clinical research for more than two decades.

A scanning laser ophthalmoscope works in the following way: a small spot is focused on the retina and is scanned in a raster pattern. An image of the retina is constructed over time by recording the scattered light and synchronizing the detected intensity with the instantaneous location of the focused spot. There are many different ways to accomplish this, but the basic concept for all scanning laser ophthalmoscopes is the same.

A scanning laser ophthalmoscope is essentially the same as a scanning laser microscope. The important difference is that, in a scanning laser ophthalmoscope, the optics of the eye always serve as the objective lens, and the sample is always the retina. While these differences may seem minor, they impose serious constraints on the imaging system. It is rare to see a system that serves as both a microscope and an ophthalmoscope (at least in the classic sense).

The main constraint that the eye imposes is its limited numerical aperture. For that reason, a SLO will never achieve the same resolution as a scanning laser microscope. The maximum possible numerical aperture of the eye (which is a measure of the steepness of the cone of focusing light) is 0.23 with an 8 mm pupil. But this is not the only problem. The benefits of increased numerical aperture for any pupil sizes larger than 2-3 mm are defeated by the presence of aberrations, which blur the image. Figure 1 shows the typical PSF of the eye as a function of pupil size. Studies have shown that the balance between diffraction which blurs the image for small pupils and aberrations is somewhere between 2 and 4 mm pupils, depending on the individual.[5,9,33] This limitation has been appreciated since the earliest SLO where a small entrance pupil less than 2 mm diameter was used to focus the scanning spot on the retina.[29]

Several attempts, such as rigid contact lenses to minimize aberrations of the cornea,[2] or judicious placement of the entrance beam to the least aberrated regions of the optical zone,[24] were made to reduce the effects of aberration but it wasn't until the use of adaptive optics that the aberration barrier was finally broken. An early adaptive optics system (to correct astigmatism only) was demonstrated by Dreher et al. in 1989 [10] but two major developments since then facilitated its effective use. The first was the implementation of a Shack-Hartmann wavefront sensor [13-14] that could quickly and reliably measure the aberrations of the eye, and the second was the integration of the wavefront sensor with a wavefront corrector, that was capable of compensating the aberrations.[15] This major development took place in David Williams' lab at the

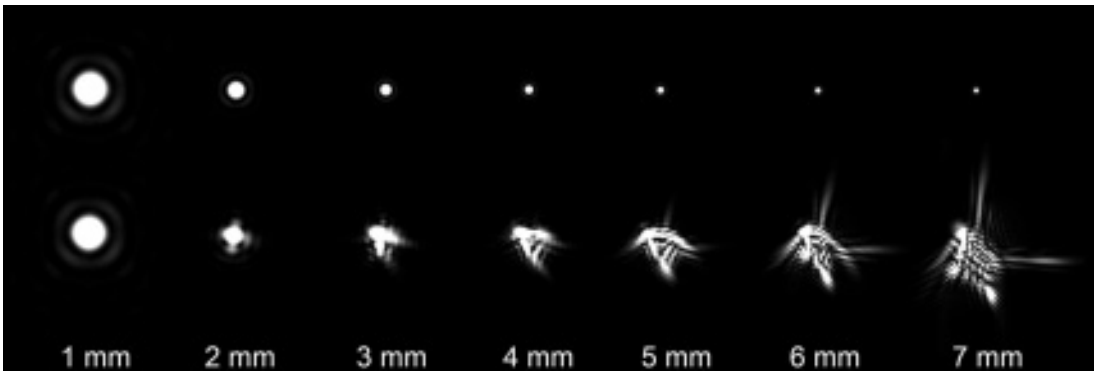

Fig. 1. The top row shows the point spread function of an eye with no aberrations. As the pupil size increases the PSF decreases in size, offering the potential for higher resolution. The lower row shows the point spread functions for an eye with typical aberrations. In this case aberrations, particularly for the larger pupil sizes, blur the PSF. The best pupil size for lateral resolution in a typical eye is between 2 and 4 mm.

University of Rochester. Their system allowed for near diffraction-limited imaging through a 6 mm pupil in a conventional flood-illuminated ophthalmoscope. The use of adaptive optics pushed resolution in living human eyes to a microscopic scale allowing, for example, direct visualization of individual cone photoreceptors. One the first scientific results from that instrument was the first-ever mapping of the spatial distribution of the three cone types that comprise the trichromatic cone mosaic.[27] Since that time many studies have been published.[4,6,11-12,19-20,25,28] But the full potential of adaptive optics for ophthalmoscopy had not been realized because of limitations imposed by the imaging modality that they used. The retina is a three-dimensional structure that is constantly moving, and it follows that an imaging modality that can reveal the retina's 3-D structure and that can image the retina in real-time would be useful. The confocal SLO is such an instrument. This paper focuses on the unique benefits of integrating adaptive optics into a scanning laser ophthalmoscope.

The Adaptive Optics Scanning Laser Ophthalmoscope

In 2002, our lab (then at the University of Houston College of Optometry) demonstrated and presented the first scanning laser ophthalmoscope that used adaptive optics to correct the high-order aberrations of the eye.[26] The AOSLO operates like any scanning laser ophthalmoscope except that it was specially designed and constructed to incorporate adaptive optics. Specifically, the system was designed to image with high pixel sampling over a small field (high magnification) and the system was designed to take advantage of AO by using a large 5.9 mm pupil for both the ingoing and outgoing beams. Adaptive optics was integrated into the path in such a way to correct the beam going into and out of the eye. The wavefront sensor was integrated in such a way that allowed us to use the same light source for wavefront sensing as was used for imaging. Mirrors were used throughout the double-pass part of the system to keep the system achromatic and to prevent back reflections from reaching the wavefront sensor or the detector. The specifications of the instrument are listed in table 1 and a schematic of the AOSLO is shown on figure 2.

Tab. 1. Specifications of the AOSLO system.

Image Sampling Density	512 X 480 pixels
Field Size	1 X 1 to 3 X 3 degrees
Wavelength	660 nm, 532 nm (any fiber coupled laser of any wavelength can be used provided that it is in the detection bandwidth of the detector)
Detector	Photomultiplier tube module (model H7422-20, Hamamatsu Corp, Japan)
Frame rate	30 frames per second
Wavefront Sensor	Shack Hartmann
effective sampling density	332 nm lenslet diameter, square array (Adaptive Optics Inc)
lenslet focal length	24 mm
Wavefront Corrector	37 actuator deformable mirror (Xinetics, Inc. Devens MA)
Laser Modulation	50 MHz bandwidth Acousto-optic modulator (Brimrose Corp, Baltimore MD)

Theoretical and practical resolution limits

The use of a confocal pinhole is an effective way to obtain high contrast retinal images, as well as to confer the ability to do optical sectioning of retinal tissue. The role of the confocal pinhole is to block scattered light from all layers except the plane of focus. An illustration of how the confocal pinhole works is shown on figure 3.

Lateral resolution

When extremely small confocal pinholes are used, lateral resolution can actually be improved beyond the conventional diffraction limit,[35] but because of light detection limits, this is a con-

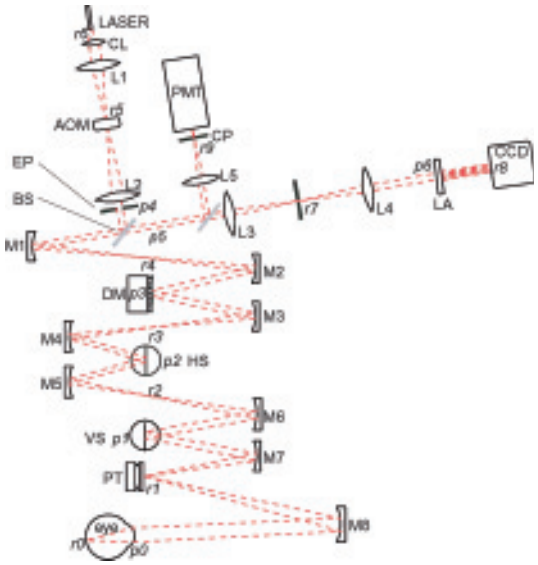

Fig. 2. Schematic of an Adaptive Optics Scanning Laser Ophthalmoscope (not to scale). The specific labeled elements are: CL - collimating lens; AOM - acousto-optic modulator; EP - entrance pupil; BS1 - beamsplitter 1; DM - deformable mirror; HS - horizontal scanning mirror; VS - vertical scanning mirror; PT - pupil tracking mirror; LA - lenslet array; CP - confocal pinhole; PMT - photomultiplier tube. Pupil conjugates and retinal conjugates are labeled *p* and *r* respectively. Mirrors and lenses are labeled *M#* and *L#* though the optical path. Telescope mirror/lens-pairs for relaying the pupil through the path are *L1-L2, L3-L4, M1-M2, M3-M4, M5-M6, M7-M8.*

dition that will not often be achieved in a SLO. From a practical standpoint, the lateral resolution is largely mediated by the sharpness of the focused beam on the way into the eye, which is why the use of AO is important. By correcting the aberrations, near diffraction-limited imaging can be achieved through larger pupils. After correcting aberrations, lateral resolutions on the order of 2 micrometers can be achieved, allowing the instrument to resolve single cone photoreceptors. Higher resolution also means higher contrast of small features, so features like capillaries and the flow of white blood cells can be resolved.

Axial resolution

Axial resolution is governed by the quality of the focused spot on the retina, the quality of the image of the focused spot at the confocal pinhole, and the size of the confocal pinhole. Axial resolution limits have been defined for diffraction limited confocal SLOs for a range of pinhole sizes,[35] for aberrated systems with tiny confocal pinholes,[9] and most importantly for aberrated systems with finite pinholes.[32] The latter case is most relevant for the AOSLO because not all aberrations are corrected by AO and finite pinholes must be used to increase signal. A summary of the Venkateswaran et al.[32] paper is shown on figures 4 A and B. The axial resolution is defined as the full width at half maximum (FWHM) of the average intensity of a planar diffuse object that is moved through the plane of focus. It is a measure of the minimum axial separation that two layers can be separated by and still be resolved. The peak intensity indicates the amount of light from a planar diffuse object that is located in the focal plane. The graphs show that axial resolution as low as 30 micrometers can be achieved as long as the aberrations are well corrected and the pinhole size is small.

To summarize the resolution improvements, the use of AO allows for a more compact focused PSF both for going into the eye (to form a compact focused spot on the retina) and for going out of the eye (to form a sharp image of the focused spot on the retina at the confocal pinhole). By making the spot smaller with AO, the pinhole size can be made smaller without too much cost

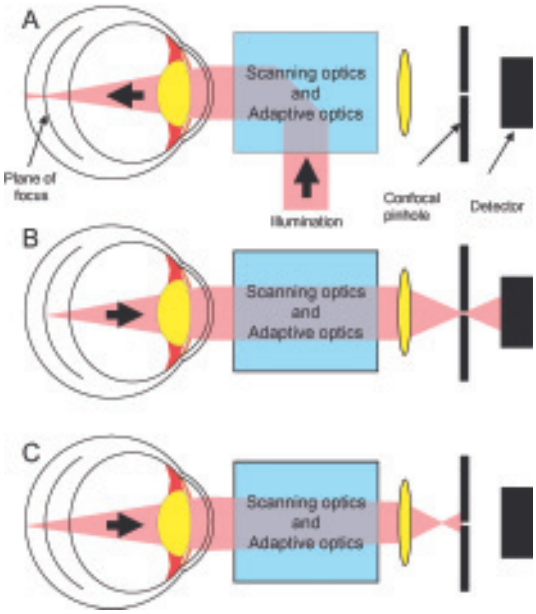

Fig. 3. Schematic to illustrate optical sectioning in a confocal scanning laser ophthalmoscope. In the illumination path (A) the light is focused to a specific plane in the retina. Although the light is focused to a plane, the incident light will scatter from all layers of the retina. Light that scatters from the plane of focus (B) passes through the optical system and is focused to an aerial image, where the confocal pinhole is placed. Light from the focal plane passes through the confocal pinhole and contributes to forming the image. Light that scatters from deeper layers (or more anterior layers) (C) is re-imaged in a plane other than the confocal pinhole plane which blocks it from reaching the detector. The confocal pinhole limits the light in the image to only what originates from the scattered light near the plane of focus.

in detected light. The smaller confocal pinhole allows for improved contrast and increased axial resolution.

RESULTS

Benefits of using adaptive optics

Based on the previous section, one expects a triple benefit of using adaptive optics in a scanning laser ophthalmoscope: first the resolution should improve because the focused spot is made more compact with AO. Second the intensity of the image should increase because more light from the focused spot on the retina is focused through the pinhole. Finally, as the axial section gets narrower, the contrast of the in-focus retinal features should increase. All of these improvements are apparent in the pair of images shown on figure 5.

Dynamic imaging

A feature of the AOSLO that is difficult to appreciate in this paper is that the AOSLO is a real-time imaging system, operating at 30 frames per second. The practical advantage of real-time imaging over taking snapshots when imaging with a small field size is the immediate feedback, which makes it much easier to navigate around the retina. But the scientific and clinical benefits are most useful. With AO-corrected real-time images we are able, without relying on contrast agents like fluorescein, to visualize blood flow through the smallest capillaries in the retina.[17] Unlike Doppler systems, which are most sensitive for high velocities, the AOSLO is most effective at measuring the slowest velocities and lowest flow rates in the retina, which are found in the smal-

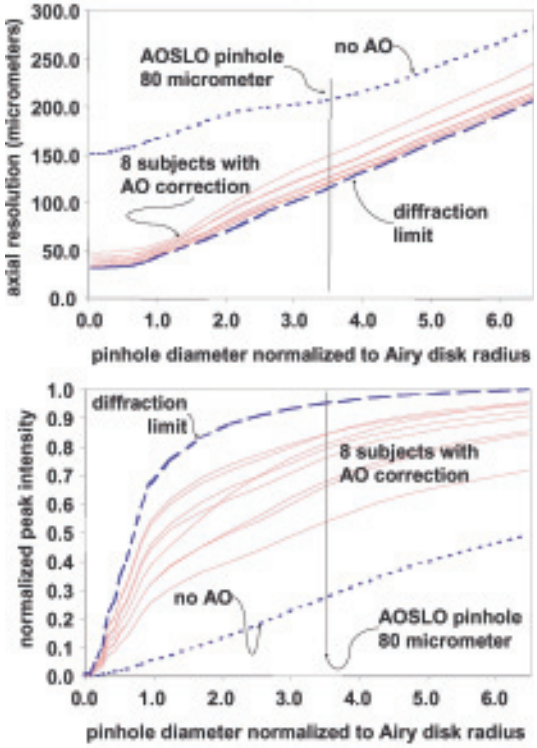

Fig. 4. These are results from a simulation of axial resolution (a) and detected intensity (b) as a function of aberration correction and pinhole diameter. By correcting most of the aberrations, resolution approaches the diffraction limit but residual aberrations still limit the amount of detectable light passing through the pinhole.

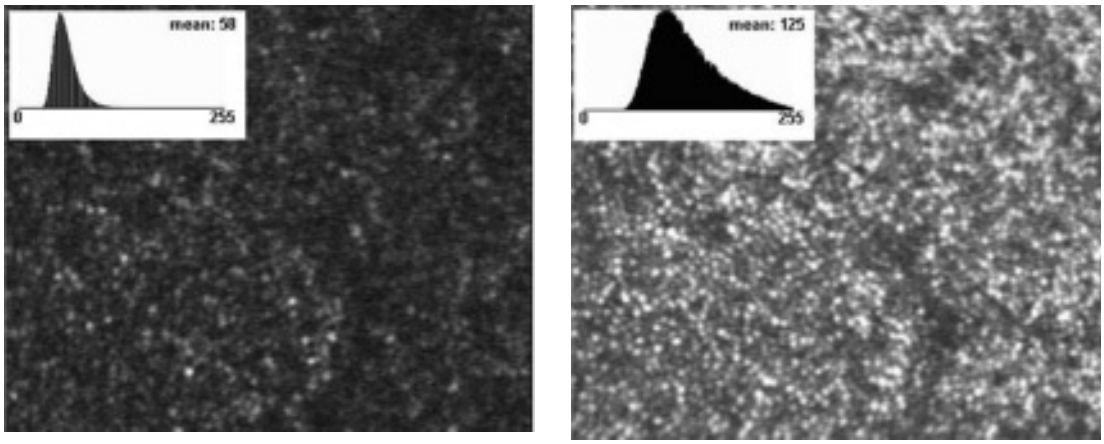

Fig. 5. The two figures show the same area of retina taken with and without aberration correction with AO. In this case, the root mean square wavefront error was reduced from 0.55 to 0.10 μm. The insets show the histograms of gray scales in the image.

lest capillaries. The capillaries that carry the blood flow are also visualized, so the exact source of the flow signal is unambiguous. Furthermore, unperfused, or ''ghost capillaries'', can also be seen. Such measurements may find important applications for tracking, treatment and under-

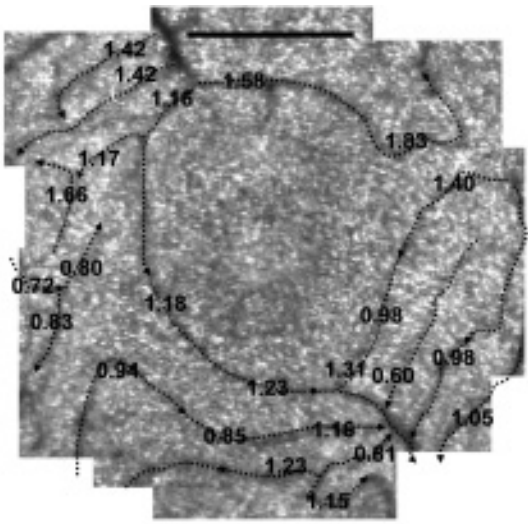

Fig. 6. This figure is a composite of a series of registered AOSLO frames. The average velocity was measured in all capillaries at the edge of the foveal avascular zone. The velocities in mm/sec are overlayed on each capillary. The scale bar indicates one degree or about 300 microns.

standing of diabetes, where irregularities in the blood flow can lead to profound complications near the fovea. Figure 6 shows an image of the parafoveal region with leukocyte velocities in mm/second superimposed.

Axial sectioning

Although conventional confocal SLOs like the Heidelberg Retinal Tomograph (Heidelberg Engineering, Germany) have used the axial sectioning capability to scan through different layers of the retina, the resolution has always been limited by the aberrations of the eye to about 300 microns.[3] Adaptive optics pushes the resolution to a level that makes it possible to obtain high transverse resolution images of independent retinal layers. Figure 7 shows a through-focus image series of a section of retina, which is indicated by the yellow square in the conventional photo. The series spans layers from the photoreceptors to the inner limiting membrane. Experimental quantification of the axial resolution was measured by recording the scattered light intensity from different retinal features (photoreceptors and blood vessels) for a range of focus positions.[23] Figure 8 is a graph showing typical through-focus intensity plots for different pinhole sizes. The FWHM values are close to theoretical expectations (Fig. 4). Axial resolution measured from the blood vessel actually exceed the theoretical expectations, likely because the blood vessel has specular or mirror-like scattering properties. We have measured axial resolutions as low as 70 micrometers with 50 micrometer pinholes (2.18 normalized units on figure 4) and 100 micrometers for 80 micrometer pinholes (3.48 normalized units on figure 4).

Clinical imaging

The noninvasive aspect of the AOSLO opens the possibility of using the instrument as a clinical tool. The high contrast and high resolution allows us to see features that are not detectable by conventional clinical tests. Here we show a couple of examples.

Diabetic retinopathy

A 35-year-old male with history of Type 1 Diabetes Mellitus (22 years) and Mild Non-Proliferative Diabetic Retinopathy was imaged using the AOSLO. A fundus exam revealed minimal exu-

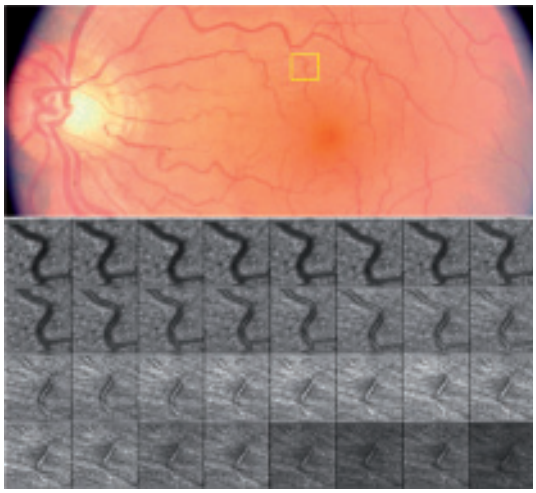

Fig. 7. The upper figure shows the left eye of a normal subject with a yellow square indicating the position and size of the AOSLO field. The lower part of the figure is a series of through-focus optical sections starting at the photoreceptor layer (upper left) and moving anteriorly through the nerve fiber layer. The separation between each layer is about 10 micrometers.

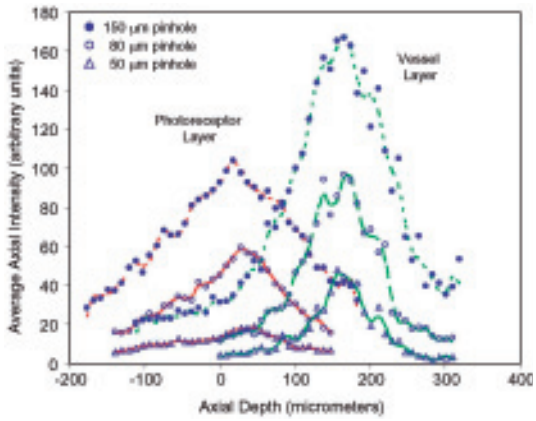

Fig. 8. Through focus intensity profiles of photoreceptors (left curves) and a blood vessel (right curves). Plots are shown for three different pinhole sizes. As the pinhole size decreases, the overall intensity decreases, but the axial resolution increases.

dates temporal to the fovea with few microaneurysms. The remaining perifoveal area appeared normal by fundus photography (Fig. 9 A). AOSLO imaging of the perifoveal area revealed the presence of microscopic capillary abnormalities in the normally appearing retina (area M, Fig. 9 A and Fig. 9 B). Serial imaging of the hard exudates with the AOSLO over a period of six months detected microscopic variations in the distribution of the hard exudates which would have been harder to measure by other means (Fig. 9 C). The high resolution of the AOSLO allowed the detection of these early vascular changes induced by diabetes.

Solar retinopathy

A 32-year-old male astronomer was accidentally exposed to direct sunlight while taking pictures of a solar eclipse in 1995. He was unaware that there had been any retinal damage. His visual acuity was 20/20 on a routine exam. An Amsler grid exam did not detect any scotomas. Fun-

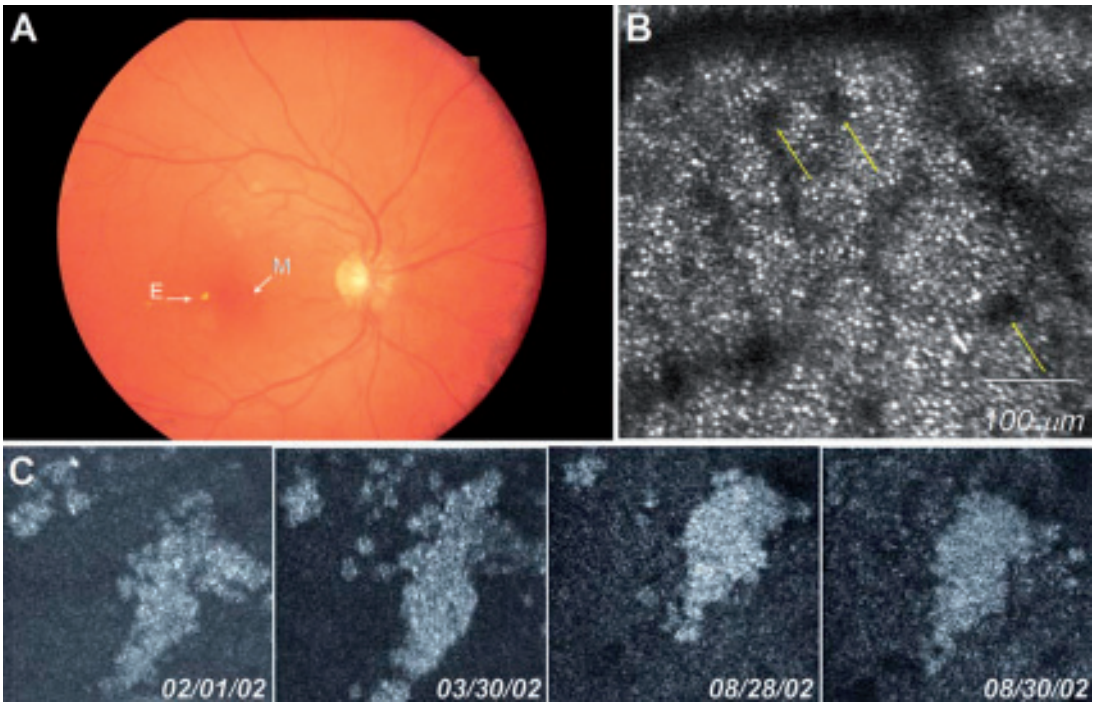

Fig. 9. A. Fundus photograph with E representing a hard exudates, and M representing the area where microaneurysms were detected with AOSLO. B. Capillary microaneurysms seen with AOSLO (M on fundus photograph) and the lower series. C. On the bottom documents the microscopic change in size of the hard exudates (E on fundus photograph), imaged with AOSLO over a period of six months.

duscopy (Fig. 10 A) and fluorescein angiography (Fig. 10 B) revealed no abnormalities. Optical Coherence Tomography (OCT 3) was performed through the scotoma, but no remarkable change in the photoreceptor or RPE layer was seen (Fig. 10 C). AOSLO video and images, which revealed a well-delineated, hyporeflective region in the perifoveal area (Fig. 10 D), was the only method that could see anything. The burn was likely missed with conventional imaging and with FA because of the presence of the foveal reflex combined with the lower contrast that these methods face in the highly pigmented foveal region. The reason why OCT failed to detect the burn is unknown, but it is possible that the photoreceptor cell layer is intact but is not waveguiding properly. In this example, the AOSLO offers a better imaging modality than other methods.

More than just imaging

To say that an SLO is simply a different imaging modality is a major understatement. The SLO goes way beyond an imaging tool. To appreciate this, you need not look any further than the publications of the inventors who appreciated the ramifications of the technology from the onset.[34] The raster scanning beam can be modulated or manipulated to paint any picture or deliver any raster scanned stimulus to the retina. Moreover, the SLO has the ability to simultaneously image the retina, containing the stimulus that is delivered. This unique ability facilitates measurements like microperimetry, localized measures of acuity, therapeutic laser delivery, fixation monitoring and fixation stability.[16,31,36]

The AOSLO has all the same features as a conventional SLO, but its ability to present a sharp image to the retina and determine its precise location from the recorded image is unprecedented. The addition of AO opens the opportunity to explore the neural limits of vision, by overcoming blur from the optics. To take advantage of the AO correction, we had to develop a light deliv-

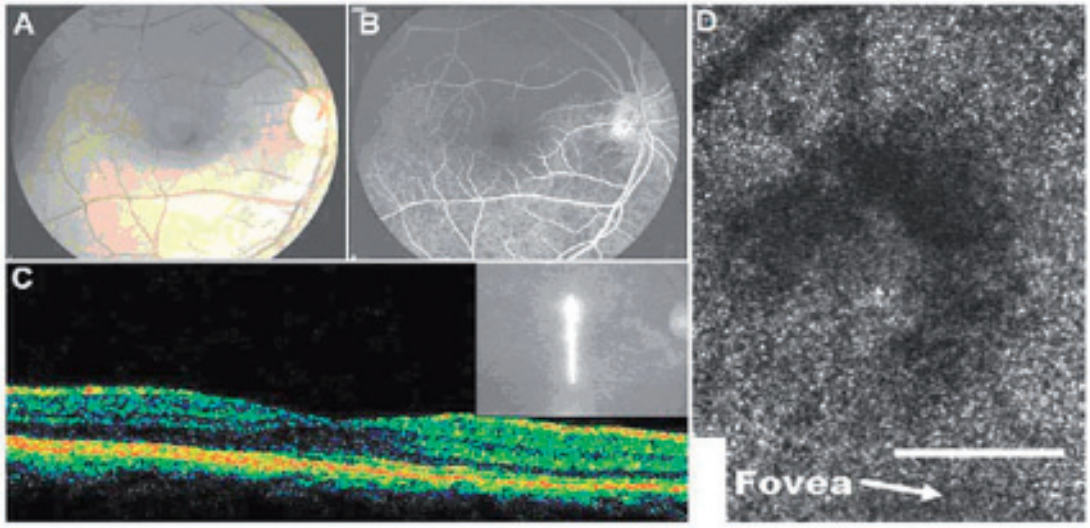

Fig. 10. A. Fundus photograph. B. Fluorescein angiogram. C. Vertical OCT scan through the affected area revealing no obvious damage. D. AOSLO revealing a hyporeflective spot as close as 100 micrometers from the fovea corresponding to a loss of waveguiding photoreceptors due to direct exposure to sunlight (scale bar on AOSLO image is 100 micrometers)

ery system that had higher bandwidth and precision than the imaging system itself. To that end, we employed a waveform generator whose output was connected to a high bandwidth acousto-optic modulator. The waveform generator was driven by a pixel clock, which was driven by the hsync from the SLO system. The bandwidth of the light delivery system was 50 MHz, which exceeded the pixel sampling frequency of 20 MHz. As a result, we could control a stimulus with a resolution that exceeded the pixel density of the image. Considering that the pixel size for a 1.5 degree field is about 0.8 micrometers, it is possible to deliver stimuli on the scale of a single cone - only limited by the resolution of the eye. The system is also able to project any predefined series of frames, or animations to the retina. Figure 11 shows a single frame containing a high resolution image exposed by the stimulus. In this image, the quality is poorer than other still frames because it is comprised of a single frame, rather than a registration of multiple frames. In a demonstration experiment, we recently measured visual acuity (VA) with the system and found an average VA of 20/11.1 for an AO-corrected 5.9 mm pupil (four-alternative forced-choice tumbling E acuity test, VA determined as the letter size corresponding to a 72.4 % number of correct responses based on a Weibull fit to a psychometric function).[22]

Another feature of the SLO is possible because of the fact that it acquires an image over time by recording the scattered light from a focused spot as it scans in a raster pattern on the retina. With this type of imaging, there is a time difference between the acquisition of the top of the image compared to the bottom. If the eye moves during that time, the image is not blurred, but rather it gets distorted in specific ways depending on the direction of motion.[7,18,29] While this causes problems when one tries to register and add multiple frames, it also offers a unique method to record eye movements. In a sense, each frame of the AOSLO is like a short chart record of the eye movements; it is just a matter of developing the tools to extract the movement signal from the image. With the AO image, the potential exists to recover eye movements with a resolution on the spatial scale of a single cone and a frequency that is many times the frame rate of the system. These efforts have recently been demonstrated.[30] The advantage of such a process is that once the eye movements are recovered, the trace can be used to remove the distortion in each AOSLO frame, making it possible to register and add multiple frames to increase signal to noise in the images. The ability to add multiple frames is important for the AOSLO because the

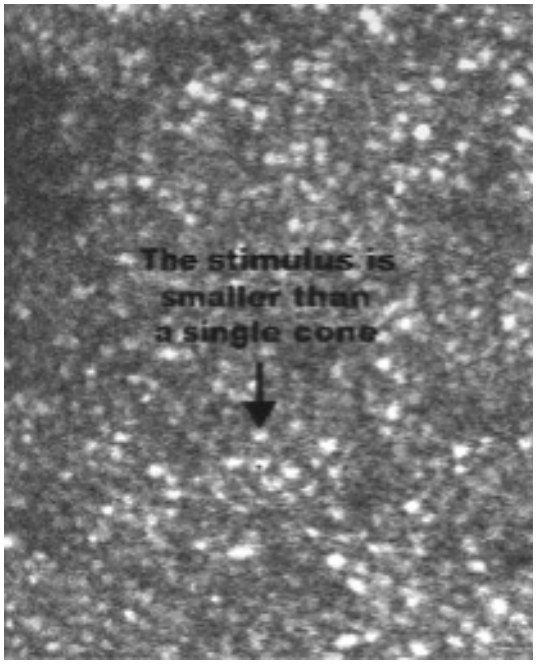

Fig. 11. This is a single AOSLO frame. The image spans a 0.58 × 0.78 degree patch of retina about 3 degrees temporal to the fovea. The stimulus delivered (which comprises the text, the arrow and the small spot) is visible to the subject, and is also observed directly on the image. The sharpness of the stimulus is limited only by the pupil size and quality of the AO-correction. The small black spot stimulus can be made small enough to fall on a single cone, and the exact cone that was stimulated can be determined from the video.

continuous exposure and small field size impose limits on the maximum amount of exposure can be used.[1] These limited exposures, combined with the fact that we use the smallest possible pinholes for enhanced contrast, yield low detected light levels, which result in single frames with low signal-to-noise.

CONCLUSION

Adaptive optics have already been proven as an effective tool for microscopic imaging of living human retina. The clinical benefits of this new view of the retina are beginning to be realized. But the broad potential applications of the technology will only be realized after getting these instruments into the hands of more clinicians and basic scientists. To that end, smaller and less expensive technology, such as MEMS deformable mirrors,[8] are being designed and tested. Also, with more experience, we are learning how to make these instruments more robust and user-friendly.

ACKNOWLEDGEMENTS

This work was funded by the National Institutes of Health Bioengineering Research Partnership Grant EY014375 and the National Science Foundation Science and Technology Center for Adaptive Optics, managed by the University of California at Santa Cruz under cooperative agreement #AST-9876783.

REFERENCES

(1) ANSI – American National Standard for the Safe Use of Lasers ANSI Z136.1-2000. Laser Institute of America, Orlando FL 2000
(2) BARTSCH D.U., ZINSER G., FREEMAN W.R. – Resolution improvement in confocal scanning laser tomography of the human fundus. Vision Science and its applications: technical digest (OSA, Washington, DC). 1994; 134-137
(3) BIRNGRUBER R., SCHMIDT-ERFURTH U., TESCHNER S., NOACK J. – Confocal laser scanning fluorescence topography: a new method for three-dimensional functional imaging of vascular structures. Graefe's Arch Clin Exp Ophthalmol 2000; 238: 559-565
(4) BRAINARD D.H., ROORDA A., YAMAUCHI Y., CALDERONE J.B., METHA A.B., NEITZ M., NEITZ J., WILLIAMS D.R., JACOBS G.H. – Functional consequences of individual variation in relative L and M cone numerosity. J Opt Soc Am A 2000; 17: 607-614
(5) CAMPBELL F.W., GUBISCH R.W. – Optical quality of the human eye. J Physiol 1966; 186: 558-578
(6) CARROLL J., NEITZ M., HOFER H., NEITZ J., WILLIAMS D.R. – Functional photoreceptor loss revealed with adaptive optics: an alternate cause of color blindness. Proc Natl Acad Sci USA 2004; 101: 8461-8466
(7) CORNSWEET T.N. – New technique for the measurement of small eye movements. J Opt Soc Am 1958; 48: 808-811
(8) DOBLE N., YOON G., BIERDEN P., CHEN L., OLIVIER S., WILLIAMS D.R. – Use of a microelectromechanical mirror for adaptive optics in the human eye. Optics Letters 2002; 27: 1537-1539
(9) DONNELLY III W.J., ROORDA A. – Optimal pupil size in the human eye for axial resolution. J Opt Soc Am A 2003; 20: 2010-2015
(10) DREHER A.W., BILLE J.F., WEINREB R.N. – Active optical depth resolution improvement of the laser tomographic scanner. Appl Opt 1989; 28: 804-808
(11) HOFER H., CARROLL J., NEITZ J., NEITZ M., WILLIAMS D.R. – Organization of the human trichromatic cone mosaic. J Neurosci 2005; 25: 9669-9679
(12) HOFER H., SINGER B., WILLIAMS D.R. – Different sensations from cones with the same pigment. J Vision 2005; 5: 444-454
(13) LIANG J., GRIMM B., GOELZ S., BILLE J.F. – Objective measurement of wave aberrations of the human eye with use of a Hartmann-Shack wave-front sensor. J Opt Soc Am A 1994; 11: 1949-1957
(14) LIANG J., WILLIAMS D.R. – Aberrations and retinal image quality of the normal human eye. J Opt Soc Am A 1997; 14: 2873-2883
(15) LIANG J., WILLIAMS D.R., MILLER D. – Supernormal vision and high-resolution retinal imaging through adaptive optics. J Opt Soc Am A 1997; 14: 2884-2892
(16) MAINSTER M.A., TIMBERLAKE G.T., WEBB R.H., HUGHES G.W. – Scanning laser ophthalmoscopy: clinical applications. Ophthalmol 1982; 89: 852-857
(17) MARTIN J.A., ROORDA A. – Direct and non-invasive assessment of parafoveal capillary leukocyte velocity. Ophthalmology 2005; 112: in press
(18) MULLIGAN J.B. – Recovery of motion parameters from distortions in scanned images. Proceedings of the NASA Image Registration Workshop (IRW97). NASA Goddard Space Flight Center, Greenbelt MD 1997
(19) NEITZ J., CARROLL J., YAMAUCHI Y., NEITZ M., WILLIAMS D.R. – Color perception is mediated by a plastic neural mechanism that is adjustable in adults. Neuron 2002; 35: 783-792
(20) PALLIKARIS A., WILLIAMS D.R., HOFER H. – The reflectance of single cones in the living human eye. Invest Ophthalmol Vis Sci 2003; 44: 4580-4592
(21) POMERANTZEFF O., WEBB R.H. – Scanning ophthalmoscope for examining the fundus of the eye. US Patent 1980; 4: 213,678
(22) POONJA S., PATEL S., HENRY L., ROORDA A. – Dynamic visual stimulus presentation in an adaptive optics scanning laser ophthalmoscope. J Refract Surg 2005; 21: S575-S580
(23) ROMERO-BORJA F., VENKATESWARAN K., ROORDA A., HEBERT T.J. – Optical slicing of human retinal tissue in vivo with the adaptive optics scanning laser ophthalmoscope. Appl Opt 2005; 44: 4032-4040
(24) ROORDA A., CAMPBELL M.C.W., CUI C. – Optimal entrance beam location improves high resolution retinal imaging in the CSLO. Invest Ophthalmol Vis Sci Suppl 1997; 38: 1012 (abstract 4708)
(25) ROORDA A., METHA A.B., LENNIE P., WILLIAMS D.R. – Packing arrangement of the three cone classes in primate retina. Vision Res 2001; 41: 1291-1306

(26) ROORDA A., ROMERO-BORJA F., DONNELLY W.J., QUEENER H., HEBERT T.J., CAMPBELL M.C.W. - Adaptive optics scanning laser ophthalmoscopy. Optics Express 2002; 10: 405-412
(27) ROORDA A., WILLIAMS D.R. – The arrangement of the three cone classes in the living human eye. Nature 1999; 397: 520-522
(28) ROORDA A., WILLIAMS D.R. – Optical fiber properties of individual human cones. J Vision 2002; 2: 404-412
(29) STETTER M., SENDTNER R.A., TIMBERLAKE G.T. – A novel method for measuring saccade profiles using the scanning laser ophthalmoscope. Vision Res 1996; 36: 1987-1994
(30) STEVENSON S.B., ROORDA A. – Correcting for miniature eye movements in high resolution scanning laser ophthalmoscopy. In: Manns F., Soderberg P., Ho A. (eds.) Ophthalmic Technologies XI. SPIE, Bellingham WA 2005; 145-151
(31) VARANO M., SCASSA C. – Scanning laser ophthalmoscope microperimetry. Semin Ophthalmol 1998; 13: 203-209
(32) VENKATESWARAN K., ROORDA A., ROMERO-BORJA F. – Theoretical modeling and evaluation of the axial resolution of the adaptive optics scanning laser ophthalmoscope. J Biomed Opt 2004; 9: 132-138
(33) WALSH G., CHARMAN W.N., HOWLAND H.C. – Objective technique for the determination of monochromatic aberrations of the human eye. J Opt Soc Am A 1984; 1: 987-992
(34) WEBB R.H., HUGHES G.W., POMERANTZEFF O. – Flying spot TV ophthalmoscope. Appl Opt 1980; 19: 2991-2997
(35) WILSON T. – The role of the pinhole in confocal imaging systems. In: Pawley J.B. (ed.) The handbook of biological confocal microscopy. Plenum Press, New York NY 1990; 99-113
(36) WORNSON D.P., HUGHES G.W., WEBB R.H. – Fundus tracking with the scanning laser ophthalmoscope. Appl Opt 1987; 26: 1500-1504

.....

Corresponding address:

Austin Roorda PhD
School of Optometry
University of California, Berkeley
Room 485 Minor Hall
Berkeley, CA 94720
UNITED STATES
Phone: (510)642-2380
Email: aroorda@berkeley.edu